Sensitivity of ocean carbon tracer distributions to particulate organic flux parameterizations

M. T. Howard,[1] A. M. E. Winguth,[1] C. Klaas,[2] and E. Maier-Reimer[3]

Received 28 February 2005; revised 14 February 2006; accepted 30 March 2006; published 4 August 2006.

[1] Vertical fluxes of particulate organic carbon (POC) from the euphotic zone to the deep sea are an important part of the carbon cycle in the oceans. In this study, oceanic fluxes of POC below the euphotic zone were simulated with the Hamburg ocean carbon cycle model (HAMOCC5.1) by using different POC-flux parameterizations and compared with sediment trap data. Overall, the geochemical distributions in the deep sea showed a high sensitivity to the selection of POC flux parameterization. Below 2000 m in the oceans, differences between simulated and observed carbon tracers (PO_4, Alk*) and model-data differences of POC fluxes are lowest when a regionally variable POC flux parameterization is used. Specifically, model-data differences are lowest in the subtropics when simulated vertical POC flux considers mineral ballasting, while they are lowest in the Arabian Sea and west coast of Africa when a mineral dust parameterization is used for the vertical POC flux.

Citation: Howard, M. T., A. M. E. Winguth, C. Klaas, and E. Maier-Reimer (2006), Sensitivity of ocean carbon tracer distributions to particulate organic flux parameterizations, *Global Biogeochem. Cycles*, *20*, GB3011, doi:10.1029/2005GB002499.

1. Introduction

[2] Particulate organic carbon (POC) and the ratio of particulate inorganic carbon (PIC) to POC that sinks below the euphotic zone down to ocean sediments plays a significant role in the partitioning of carbon between the ocean and atmosphere [*Archer et al.*, 2000]. Therefore proper quantification of the export and remineralization of POC in ocean carbon cycle models and corresponding changes in POC/PIC ratios is important. Earlier studies [*Suess*, 1980; *Betzer et al.*, 1984; *Berger et al.*, 1987; *Martin et al.*, 1987, *Pace et al.*, 1987] have attempted to predict POC export from the euphotic zone as well as the depth dependence of POC fluxes by relating POC fluxes at depth to primary production or export production (defined as the POC flux at the base of the euphotic zone). The interdependence among primary production, export production and the depth dependence of POC fluxes has been reevaluated using more recent and widespread data sets [*Antia et al.*, 2001; *Lutz et al.*, 2002]. The studies of *Antia et al.* [2001] and *Lutz et al.* [2002] have revealed high geographical variability in the relationship between export production and primary production. Furthermore, the depth dependence of POC penetration profiles was shown to vary independently of export production. Several studies [e.g., *Honjo*, 1982; *Ittekkot*, 1993; *Hedges et al.*, 2001; *Armstrong et al.*, 2002; *Francois et al.*, 2002; *Passow*, 2004] have investigated the dependence of the vertical POC flux on mineral particle aggregation in the ocean, but mechanisms of this aggregation are not well known. For example, an increase in dust deposition may influence the penetration depth of POC [*Ittekkot*, 1993]. Recently, *Armstrong et al.* [2002] showed that despite high variability in POC fluxes in sediment traps, the ratios of POC flux to mineral fluxes tend to be almost constant in the deep ocean. *Armstrong et al.* [2002] proposed a partition of POC fluxes into different fractions: a free fraction remineralizing at a length scale similar to that proposed by *Martin et al.* [1987] and a mineral-associated fraction that remineralizes at length scales similar to that of the minerals. The mineral-associated fraction could be further partitioned between mineral opal, $CaCO_3$ and lithogenic material [*Klaas and Archer*, 2002]. Hence the distribution and geographical variability of POC fluxes in the deep ocean could determine the flux and composition of minerals. Conversely, the flux and composition of minerals can have an impact on POC fluxes. Because the fraction of POC associated with $CaCO_3$ is substantially higher than the fraction associated with opal, such a parameterization might preclude large variation in the PIC:POC rain ratios into the sediments. *Francois et al.* [2002] have also shown that the variability in POC fluxes at depth is related to the composition of mineral fluxes with higher POC to mineral flux ratios associated with $CaCO_3$ fluxes.

[3] The purpose of this study is therefore to test the sensitivity of the carbon cycle and PIC:POC rain ratios below the mixed layer to the different formulations of the depth dependence of POC fluxes. Specifically, the response of a 3D model of the marine carbon cycle that includes a detailed description of nutrient co-limitation (including iron) and an ecosystem dynamics parameterization that resolves the seasonal cycle is investigated. In addition we test the sensitivity

[1]Department of Atmospheric and Oceanic Sciences, University of Wisconsin-Madison, Madison, Wisconsin, USA.
[2]Alfred-Wegener-Institut für Polar- und Meeresforschung, Bremerhaven, Germany.
[3]Max-Planck-Institut für Meteorologie, Hamburg, Germany.

0886-6236/06/2005GB002499$12.00

of the model to the following parameters: remineralization rates, penetration depths (or the so-called e-folding depths) of POC, $CaCO_3$, and opal, and the PIC:POC ratio (rain ratio) of export production. The rain ratio is of considerable interest for transfer of carbon into the deep sea and has been controversially discussed [e.g., *Koeve*, 2002; *Mekik et al.*, 2002; *Sarmiento et al.*, 2002; *Balch et al.*, 2005].

2. Model Description

[4] The Hamburg ocean carbon cycle model HAMOCC5.1, used in this study, is based on work by *Maier-Reimer* [1993], *Six and Maier-Reimer* [1996], *Aumont et al.* [2003], *Heinze et al.* [2003], and *Gehlen et al.* [2003]. Its components include an NPZD ecosystem model in which primary production is limited by macronutrients (N, P, Si) and micronutrients (Fe) and a 12-layer sediment model with pore water geochemistry (see also auxiliary Text S1[1]). The model uses an Arakawa-type E-grid with approximate 3.5° × 3.5° resolution [*Maier-Reimer et al.*, 1993] and 22 vertical layers varying in thickness from 25 m at the surface to 700 m in the deepest ocean areas. Geochemical tracers are advected like tracers in the corresponding physical model with a time step of 1 month, while a shorter time step of 3 days is used in the euphotic zone (the upper two layers of the model) for the quantities varying on short timescales that determine the ecosystem processes. The relatively coarse resolution of the model allows for long-term integrations and exploration of interaction between the water column and marine sediment. The model has been integrated for 10,000 years on an NEC supercomputer at the German Climate Modeling Center (DKRZ) in Hamburg.

[5] The biogenic $CaCO_3$ (PIC) export production is parameterized as

$$P_{CaCO3} = A\left(P_{orgC} - 0.5 \cdot P_{BSi}\right), \tag{1}$$

with P_{CaCO3} the $CaCO_3$ export production (expressed in units C per unit area and unit time), P_{orgC} the export production of organic material, and P_{Bsi} the biogenic silica export production (for details, see *Heinze* [2004]). The parameter A = 0.20, which results in a global mean PIC:POC ratio of 0.175, is used as a reference value in all model simulations. This formulation implies that as long as nutrients are available, diatoms constitute the export producers (assimilating silica and carbon at a ratio of 0.5). In areas with depleted silica concentration (with P_{BSi} = 0), the PIC:POC increases according to (1) to 0.2. For equation (1), a reasonable assumption is made that most net primary production occurs in the euphotic zone. Export of POC from the euphotic zone in the reference experiment (REF) with exponentially declining uniform vertical POC is calculated according to *Gieskes* [1983],

$$\begin{aligned} \frac{\partial POC}{\partial t} &= \frac{\partial wPOC}{\partial z} - rPOC = 0 \\ \frac{\partial wPOC}{\partial z} &= \frac{\partial F_{OC}}{\partial z} = \frac{r}{w} F_{OC}, \end{aligned} \tag{2}$$

where POC is the particulate organic carbon concentration, F_{OC} the vertical POC flux, w the sinking speed of POC and r the POC remineralization rate. The quantity $w/r = z_p$ represents the e-folding length scale or "penetration depth" of POC. In the REF experiment, z_p = 1033 m.

[6] The second category of experiments (REFD) utilizes the POC flux parameterization as described above, but includes a regionally variable dependence on the atmospheric dust input similar to that described by *Ittekkot* [1993]. In this approach the penetration depth is a function of the atmospheric dust deposition

$$z_p = 200 + f\left(Fe_{input}\right), \tag{3}$$

where the regional distribution of dust is taken from an annual mean field from *Mahowald et al.* [1999]. A third category of experiments (MARTIN) uses the POC flux parameterization as described by *Martin et al.* [1987] with

$$POC(z) = POC(100\ \mathrm{m})(z/100)^{-0.858}, \tag{4}$$

which can be obtained by setting $r/w \sim 0.858/z$ in (2).

[7] The fourth category of experiments (BAL) apply a particle flux parameterization using a mineral association approach based on work by *Armstrong et al.* [2002] and *Klaas and Archer* [2002]. The total flux of organic carbon below the euphotic zone is given by

$$\begin{aligned} F_{OC} = &\left(k_{opal}\right)\left(F_{opal}(z)\right) + (k_{CaCO3})(F_{CaCO3}(z)) + (k_{lith})(F_{lith}(z)) \\ &+ F^{E}_{OC}. \end{aligned} \tag{5}$$

The vertical particle flux of organic carbon F_{OC} includes a fraction of POC that sinks in association with mineral ballast and an "excess" fraction that sinks independently of mineral ballast. The ballast-mineral associated POC fraction is determined from the mineral fluxes (F_{opal}, F_{CaCO3} and F_{lith}) and the carrying coefficients (k_{CaCO3} = 0.083, k_{opal} = 0.026, k_{lith} = 0.068) [*Klaas and Archer*, 2002]. The vertical distribution of the excess POC fraction, F^{E}_{OC}, is parameterized by equations (1) and (2) as in the REF runs but with an e-folding depth of 770 m.

[8] The POC flux associated with the mineral ballast has an e-folding depth of 2000 m for $CaCO_3$ and 4000 m for opal. Lithogenic material does not dissolve in the water column; hence all of the POC associated with lithogenic material directly sinks to the sediment.

3. Model Experiments

[9] Twelve experiments were conducted by varying parameter settings listed in Table 1 and auxiliary Table S2. Specific model-model and model-data comparisons of export production, POC fluxes, and carbon water mass tracers are given in the two following sections, 3.1. and 3.2. Focus on the data-model comparison is given for areas of high data coverage (Figure 1), i.e., the central equatorial Pacific, North Atlantic, North Pacific, Arabian Sea, and Southern Ocean.

3.1. Comparison of Simulated Export Production and POC Fluxes With Sediment Trap Data

[10] Export production is defined in this study as the amount of particulate organic carbon that sinks below the

[1] Auxiliary materials are available in the HTML. doi:10.1029/2005GB002499.

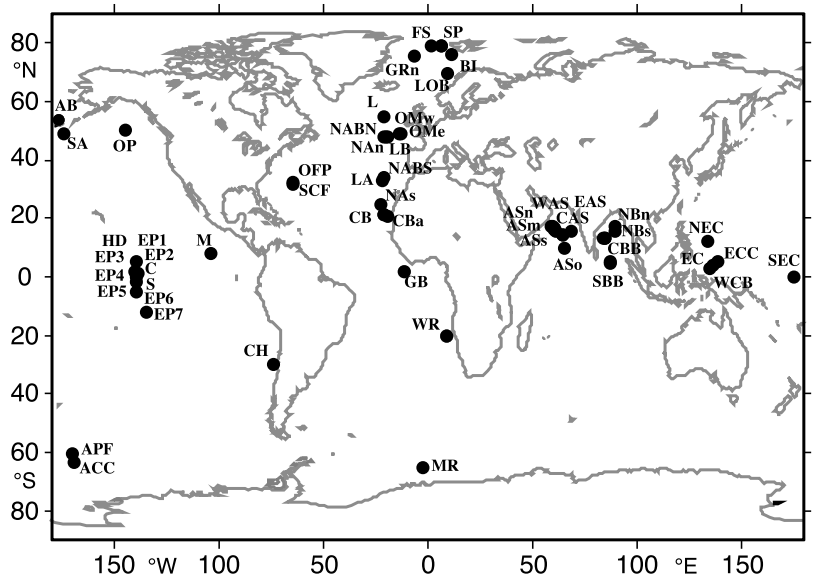

Figure 1. Locations of sediment trap data [after *Klaas and Archer*, 2002].

euphotic layers (the upper two model layers). Since nutrients are exported with POC in fixed Redfield ratios, different POC flux distributions with depth will affect the cycling of nutrients at depth and reinjection into the euphotic zone. This leads to changes in export production (Figure 2). A more effective downward POC export results in a decreased nutrient supply for the euphotic zone and thus weaker export production.

[11] The reference, experiment REF, generated an export production of 4.6 Pg C yr^{-1} and a net primary production of 27.0 Pg C yr^{-1} (Figure 2a). Highest export production rates are generated by experiment MARTIN followed by REFD, BAL and REF in decreasing order (Figure 2). In the North Atlantic, dust from the Sahara stimulates the export (Figure 2b), which yields a good match of experiment REFD to the sediment trap data (Figure 3a) (see also auxiliary Table S2). In subtropical gyres where $CaCO_3$-producing organisms favor an enhanced mineral ballasting of POC, experiment BAL generally yields a reasonable fit. For example, at 14°N 54°W (Figure 3b), $CaCO_3$-associated POC contributes significantly to the total POC flux below 2000 m (see also auxiliary Figure S3). Also in the subtropical South Atlantic (Figure 3d), there is a low model-data difference below 2000 m, with the best results obtained using the BAL formulation. In the equatorial Atlantic and Pacific, the use of a regionally variable POC flux parameterization also improves the prediction of POC fluxes (Figure 3c; see also auxiliary Table S2). In these regions, opal production dominates, but still results in lower POC fluxes above 3000 m than $CaCO_3$-associated POC because of the low carrying coefficient of opal. In the Southern Ocean, REFD matches the data well. Experiment BAL (Figure 3c; see also auxiliary Table S2) has similar distributions of export production to experiment REF in the northern hemisphere, and slightly lower in the equatorial regions and Southern Ocean (Figure 3f). Strong currents and pulsed seasonal blooms in this region increase the uncertainty in sediment trap measurements, however, especially in the upper 1000 m [*Gardner et al.*, 2000].

[12] In the Arabian Sea at 15°N 65°E (Figure 3e), annually averaged flux measurements from sediment traps show a high interannual variability, possibly due to the pulsed nature of blooms and seasonal to interannual variability of the monsoon [*Kriest*, 2002]. The different POC flux parameterization models reflect the complexity of this area for the upper 2000 m, but tend to be within the range of variability around 3000 m. Below 3000 m, trap fluxes tend to be higher than above, suggesting differences in trap efficiency or lateral transport of material. In this region, experiment REFD has the lowest model-data differences below 2000 m, possibly due to the importance of dust deposition in this region (see auxiliary Table S2).

[13] A sum of the cost function for each parameterization on sediment traps below 2000 m shows that in bathypelagic areas, the regionally varying parameterizations BAL and REFD have lower model-data differences than the regionally constant parameterizations REF and MARTIN. Experiment BAL has a 13.2% lower total cost function than REF and 12.8% lower than MARTIN, while experiment REFD has a 6.2% lower cost function than REF and a 5.7% lower cost function than MARTIN.

3.2. Effects of POC Flux Parameterization on Carbon Water Mass Tracers

[14] The simulated dissolved inorganic carbon (DIC) and phosphate distribution (Figures 4 and 5) is compared with data from the Global Ocean Data Analysis Project (GLODAP) [*Key et al.*, 2004] and World Ocean Atlas 2001 [*Conkright et al.*, 2002] (http:/www.nodc.noaa.gov OC5/WOA01F), respectively. Observed DIC is corrected by the ΔC^* method of *Gruber et al.* [1996] to remove the anthropogenic carbon perturbation (see http://cdiac.esd.ornl.gov/oceans/glodap/GlopDV.htm). The total error associated with the GLODAP data (measurement error

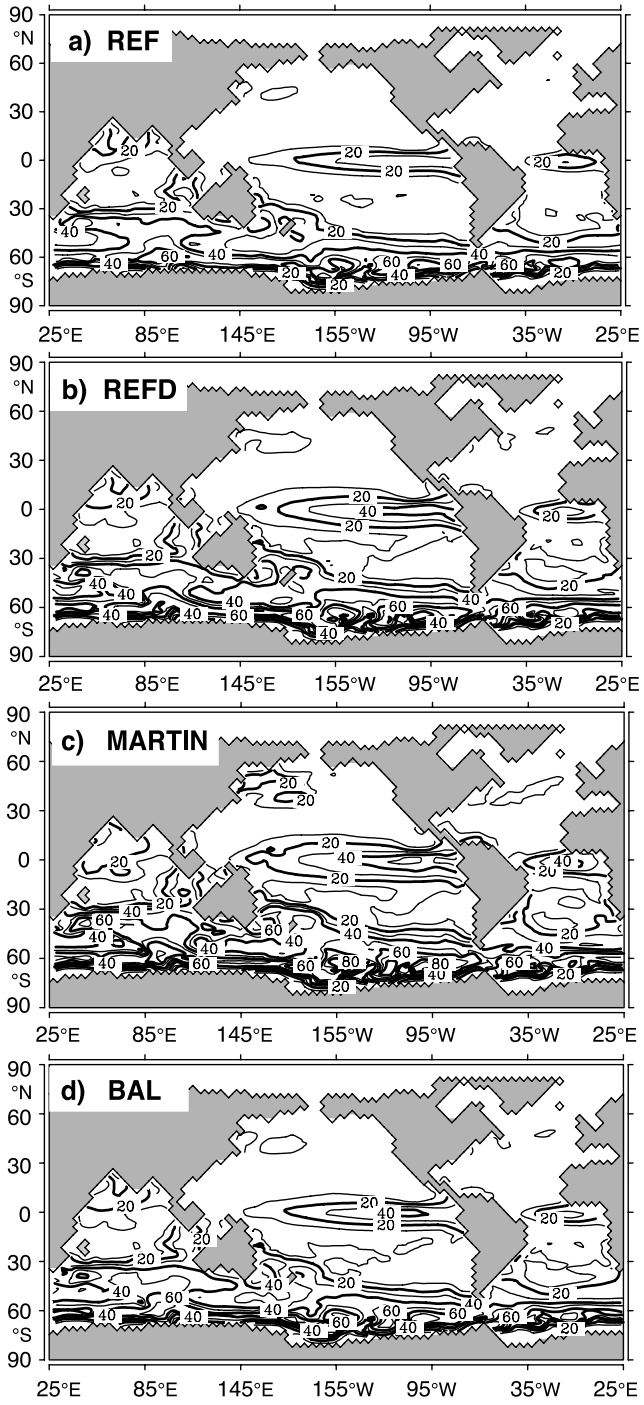

Figure 2. Simulated export production in g C m^{-2} yr^{-1} from the surface layer in the HAMOCC5.1. The contour interval in each plot is 10 g C m^{-2} yr^{-1}. All plots are from a 10,000-year model integration. (a) Experiment REF. (b) Experiment REFD. (c) Experiment MARTIN. (d) Experiment BAL.

plus the error from the anthropogenic correction) is generally between 4 and 12 μmol kg^{-1}, with highest values located in the equatorial Pacific [*Key et al.*, 2004] (see auxiliary Figure S1). The DIC difference at 3000 m between experiments and the GLODAP data is shown in Figure 4. Experiment REF (Figures 4b and 5a) has the lowest model-data difference, ranging for DIC from 30 μmol kg^{-1} in parts of the Southern Ocean to +30 μmol kg^{-1} in the central Atlantic, with near zero model-data difference in much of the central and northern Pacific. Experiments REFD (Figure 4c) and MARTIN (Figure 4d) with strong export production (Figure 3) have higher positive differences of DIC than BAL and REF as compared with GLODAP data. Experiment MARTIN has a model-data difference of up to +60 μmol kg^{-1} in the equatorial Pacific, and differences of up to +40 μmol kg^{-1} in the central Atlantic. In contrast to other experiments, simulated DIC in experiment REFD is much lower than GLODAP values (up to −40 μmol kg^{-1} in the central and North Pacific) suggesting a potential underestimate of POC fluxes using the dust parameterization. Experiment BAL (Figure 4d and 5d) is similar to REF, but with slightly higher values. Differences between BAL and GLODAP data range between −10 μmol kg^{-1} in the western Indian Ocean to around +40 μmol kg^{-1} in the North Atlantic, eastern equatorial Pacific, and parts of the Southern Ocean.

[15] Alkalinity* (Alk*) is defined to diagnose the biotic contributions to the modeled alkalinity by removing the effect of salinity,

$$Alk^* = Alk - 2340 \cdot \frac{S}{34.7}, \tag{6}$$

where Alk is the modeled alkalinity, 2340 μeq kg^{-1} is the model-mean alkalinity, S is the modeled salinity in per mil, and 34.7 is the model-mean salinity. Changes in Alk* (Figure 6) in the deep ocean are driven by calcium carbonate dissolution (increase in alkalinity) and nutrient remineralization (decrease in alkalinity). Each of the plots in Figure 6 reflects the conveyor belt circulation of the deep ocean, with lowest values of Alk* found in the North Atlantic, ranging from −125 μeq kg^{-1} in experiment MARTIN to about −40 μeq kg^{-1} in experiment BAL. The highest values of Alk* are found in the North Pacific and Indian oceans, with maximum values ranging from 20 μeq kg^{-1} in experiment REF to around 135 μeq kg^{-1} in experiment MARTIN. Experiment BAL has the lowest model-data differences in the Pacific and Indian oceans, while experiment REFD has the lowest model-data differences in the Atlantic and Southern oceans. The very high values of Alk*, up to 135 μeq kg^{-1} in experiment MARTIN in the North Pacific (Figure 6b), are a result of the high export production generated in experiment MARTIN (Figure 2). We contend that the low model-data differences of Alk* in experiments BAL and REFD show that they are producing the most realistic fluxes of PIC as compared with data, related to a higher export of silica into the deep sea and thus according to equation (1) a preference of $CaCO_3$ formation at the surface.

3.3. Sensitivity Experiments With Ballast Parameterization

[16] A series of sensitivity experiments were conducted with the ballast model (Table 1). They included (1) changing the remineralization rate of POC, (2) changing the penetration depth of $CaCO_3$, opal, and unballasted (free)

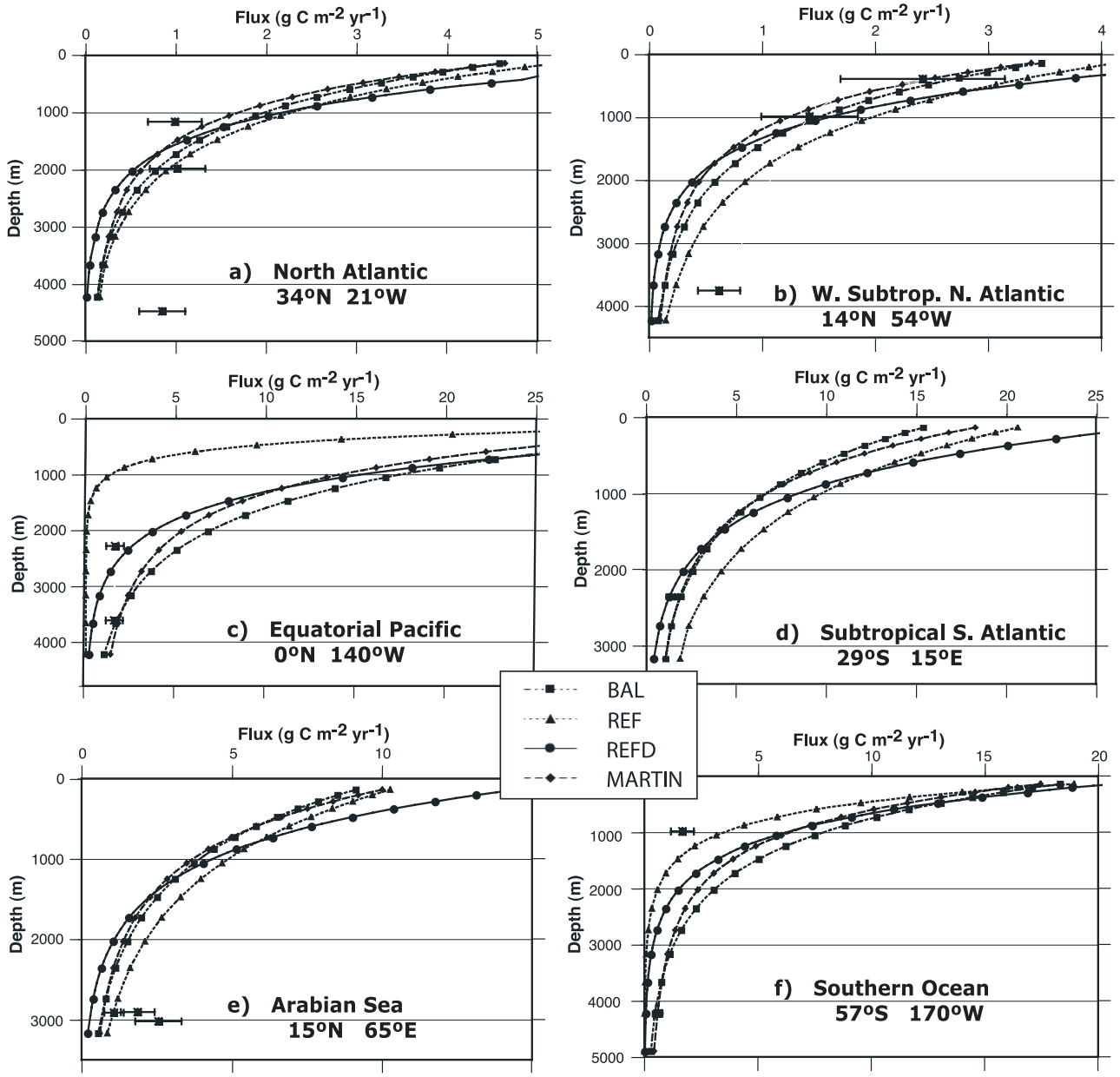

Figure 3. POC Fluxes in g C m^{-2} yr^{-1}, models compared with sediment trap data (solid squares with error bars) for experiments BAL (squares with long-short-dashed line), REF (triangles with short-dashed line), REFD (circles with solid lines), and MARTIN (diamonds with long-dashed lines). Error bars are standard 30% error on sediment trap measurements. (a) North Atlantic, 34°N, 21°W, data at 1160 m, 1980 m, and 4480 m from a Parflux 7 trap collected in 1989 and 1990 [*Honjo and Manganini*, 1993]. (b) W. Subtrop. N. Atlantic, 14°N, 54°W, data at 389 m, 988 m, and 3755 m from a Parflux 2 trap collected in 1977–1978 [*Honjo*, 1980]. (c) Equatorial Pacific, 0°N, 140°W, data at 2284 m and 3618 m from a Parflux trap collected in 1992–1993 [*Honjo et al.*, 1995]. (d) Subtropical S. Atlantic, 29°S, 15°E, data at 2516 m depth from collected in 1992–1993 [*Fischer et al.*, 2000]. (e) Arabian Sea, 15°N, 65°E, data at 2907 m, 2913 m, and 3021 m from a Parflux 6 trap collected in 1986–1988 [*Haake et al.*, 1993] and 1988–1989 [*Kempe and Knaack*, 1996]. (f) Southern Ocean, 57°S, 170°W, data at 982 m and 4224 m from a Parflux 6 trap collected in 1996–1997 [*Honjo et al.*, 2000].

POC and (3) changing the PIC:POC rain ratio below the mixed layer.

[17] In experiment BALR1, the remineralization rate was increased from 0.02 (in experiment BAL) to 0.03 per month, an increase of 50%, but with no significant changes in the distributions of carbon tracers in the water column. In experiment BALR2, remineralization was increased to 0.20 per month, an increase of 500% from experiment

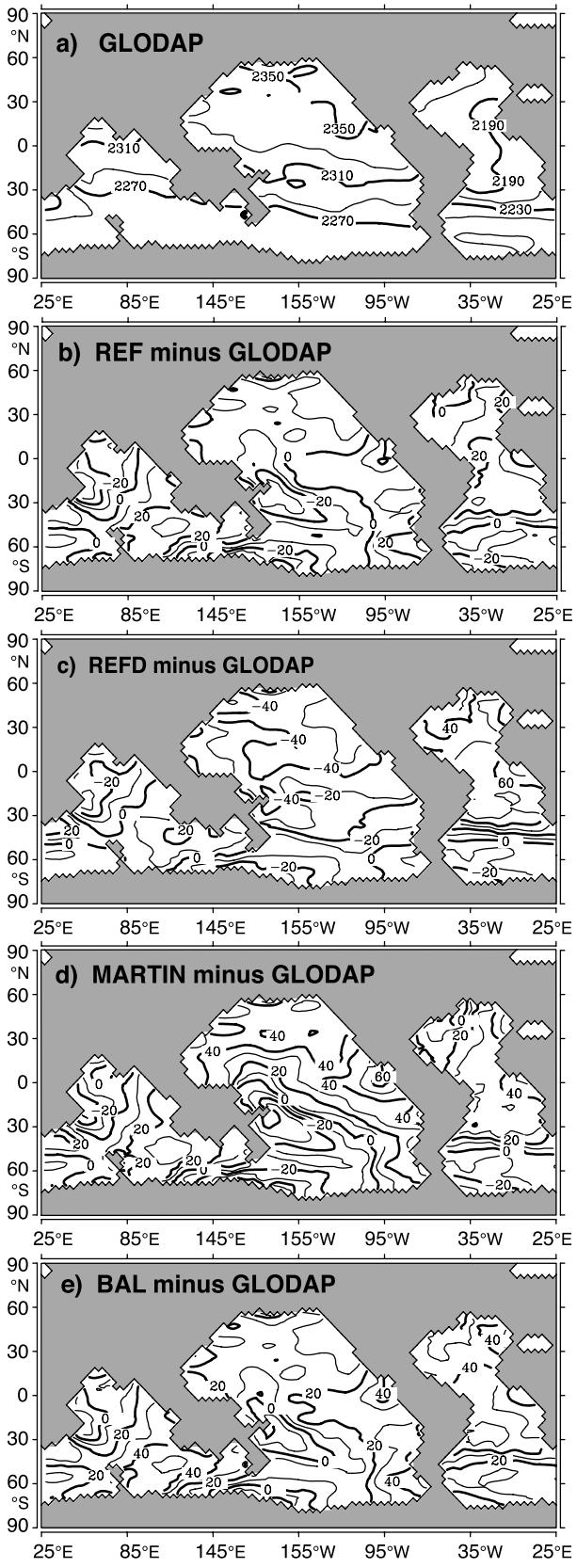

BAL, with similar results to BALR1. These experiments identified a low sensitivity of major carbon tracer distributions to POC remineralization rates.

[18] The effect of changes in e-folding depth of opal and calcite are discussed in light of experiments BALEF1 and BALEF2. In both experiments, simulated DIC distribution changed significantly from experiment BAL. In experiment BALEF1, the sinking velocity w of opal was increased by a factor of 2.5 (equation (2)). In the deep North Pacific, the difference in DIC between experiments BALEF1 and BAL is up to 30 mmol m^{-3} because of the deeper remineralization of opal-associated POC (Figure 7a). In experiment BALEF2 the sinking velocity of $CaCO_3$ (see Table 1) w was reduced by a factor of 8. The resulting DIC is increased up to 65 mmol m^{-3} relative to BAL in the deep North Pacific (Figure 7b). The changing sinking velocities of opal (BALEF1) and $CaCO_3$ (BALEF2) affect the opal and carbonate deposition to the sediments, respectively. This can alter the $CaCO_3$ deposition in the sediments and can feed back on the carbon cycle in the water column [*Archer et al.*, 2000].

[19] The average value of the PIC:POC ratio in the world ocean is still widely disputed [*Sarmiento et al.*, 2002], with estimates varying from 0.05 to 0.25. Here we test the response of the DIC and alkalinity distribution with respect to different PIC:POC ratios by changing coefficient A in equation (1) to 0.15 for experiment BALPP1 and to 0.25 for experiment BALPP2. The difference between experiment BALPP1 and BAL of Pacific alkalinity is shown in Figure 8. The alkalinity differences are up to 40 meq m^{-3} near the surface and down to -16 meq m^{-3} in areas of low oxygen concentration. The horizontal gradient of alkalinity differs significantly between these experiments through the supply of CO_3^{2-} ion from calcite dissolution, affected by the different PIC:POC ratios.

[20] In Experiment BALPP2 (Figure 8b), the results are almost exactly the opposite of those from BALPP1. The largest difference in alkalinity occurs in the surface ocean and deep South Pacific, the same as where the largest difference in total alkalinity is predicted in experiment BALPP1. The result is a net increase in the alkalinity gradients.

4. Discussion

[21] As shown in section 3, predicted POC fluxes and associated geochemical changes are sensitive to the different global and regional parameterizations of vertical carbon transport. The experiments which vary the PIC:POC ratio by varying the coefficient A in equation (1) have shown that the model generates a distribution of alkalinity with the lowest model-data difference when a coefficient of A = 0.2

Figure 4. Preindustrial distribution of DIC in μmol kg^{-1} at 3000 m depth. (a) Data from GLODAP (Global Ocean Data Analysis Project) [*Key et al.*, 2004]. (b) Experiment REF minus GLODAP data. (c) Experiment REFD minus GLODAP data. (d) Experiment MARTIN minus GLODAP data. (e) Experiment BAL minus GLODAP data. (For total error of GLODAP data, see auxiliary Figure S1).

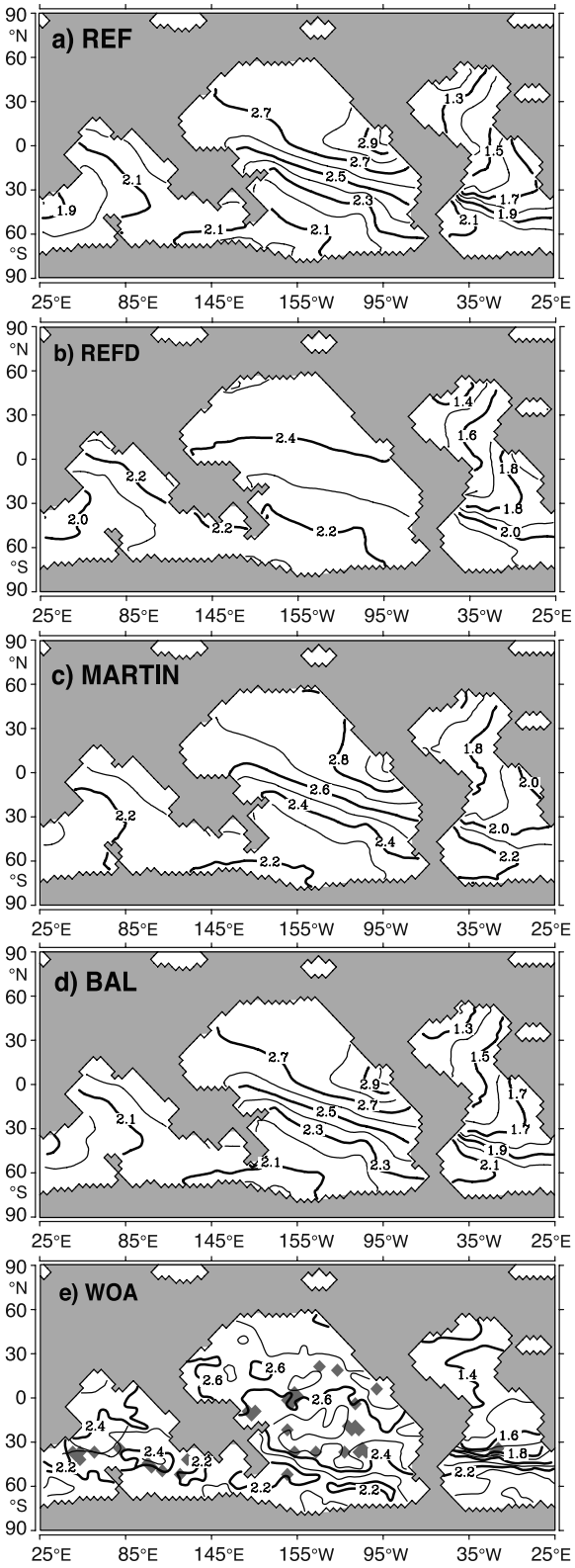

Figure 5. Model PO_4 distribution in μmol kg^{-1} at 3000 m depth normalized to WOA 2001 data with factor of 1.1925 to adjust for mass lost by sediments for experiments (a) REF, (b) REFD, (c) MARTIN, and (d) BAL. (e) For comparison, PO_4 from WOA 2001 is shown [*Conkright et al.*, 2002]. Gray areas in the ocean are areas with no data coverage.

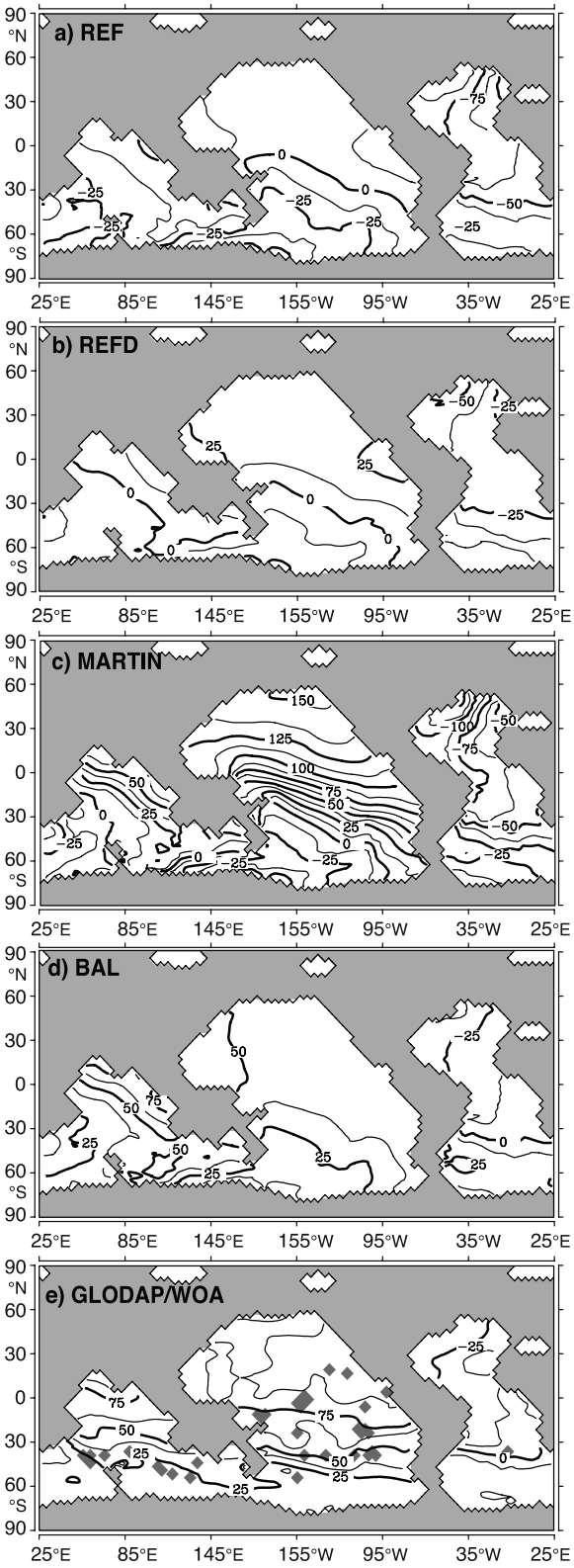

Figure 6. Alk* distribution in μeq kg^{-1} at 3000 m depth for experiments (a) REF, (b) REFD, (c) MARTIN, and (d) BAL. (e) Alk* calculated using GLODAP alkalinity data and WOA 2001 salinity data. See text for definition of Alk* (equation (6)). Gray areas in the ocean are areas with no data coverage.

Table 1. Experiment Names and Descriptions

Experiment Name	Description
REF	reference run of model before implementation of ballast parameterization; POC flux determined by constant penetration depth of 1033 m
REFD	reference run, POC flux determined by regionally variable dust input
MARTIN	reference run, utilizes Martin POC flux function of $z^{-0.858}$
BAL	baseline run of model with ballast parameterization
BALR1	remineralization rate increased to 0.03 $month^{-1}$
BALR2	remineralization rate increased to 0.20 $month^{-1}$
BALEF1	e-folding penetration depth of opal increased to 10,000 m
BALEF2	e-folding penetration depth of calcite decreased to 500 m
BALEF3	e-folding penetration depth of opal decreased to 500 m
BALEF4	e-folding penetration depth of "free" POC increased to 1000 m
BALPP1	PIC:POC ratio decreased to 0.125 ± 0.011
BALPP2	PIC:POC ratio increased to 0.225 ± 0.011

is used, generating a global mean PIC:POC of 0.175. *Koeve* [2002] suggested a global PIC:POC ratio between 0.20 and 0.25, but his findings differ substantially from the lower estimates of *Sarmiento et al.* [2002], who suggested a global average PIC:POC ratio of 0.06 ± 0.03. Results from the comparison of modeled particle fluxes with data are in general agreement with the findings of *Lutz et al.* [2002]. A main point of agreement is the finding that a regionally varying particle flux parameterization (i.e., BAL, REFD) has lower model-data differences below 2000 m than a regionally constant parameterization (i.e., REF, MARTIN). Results of this study also support the study of *Francois et al.* [2002], who suggested that a mineral ballasting parameterization should have better model-data agreement in

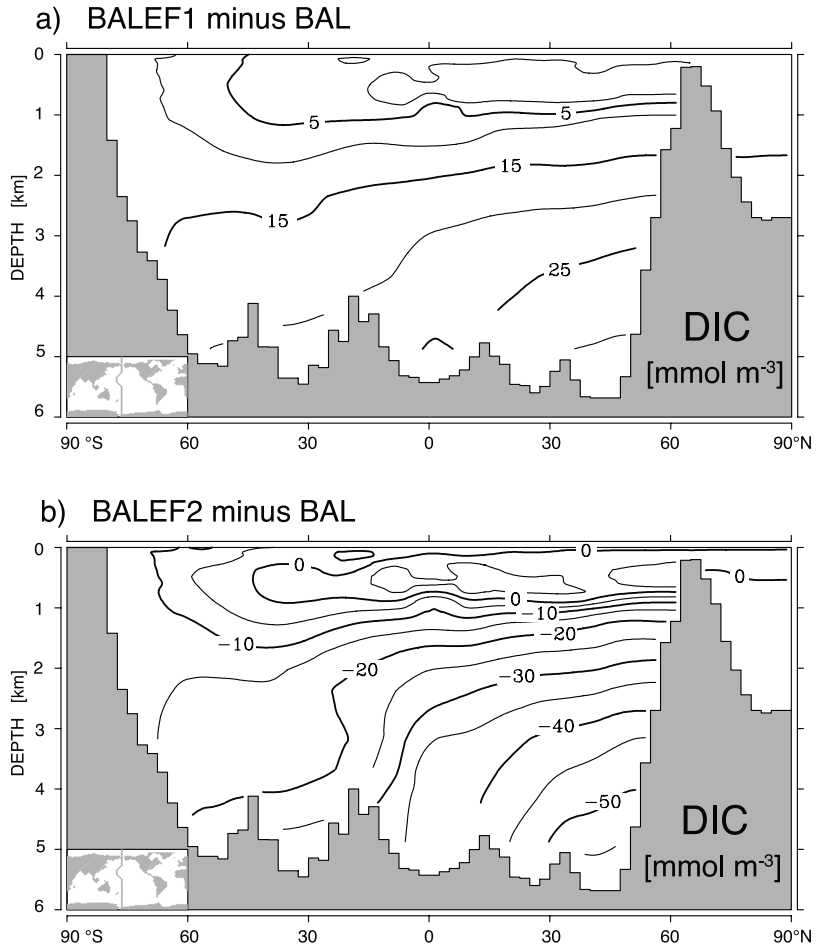

Figure 7. DIC difference plots in mmol m^{-3}. (a) Experiment BALEF1 minus Experiment BAL, Pacific section, 160°W. (b) Experiment BALEF2 minus BAL, Pacific section.

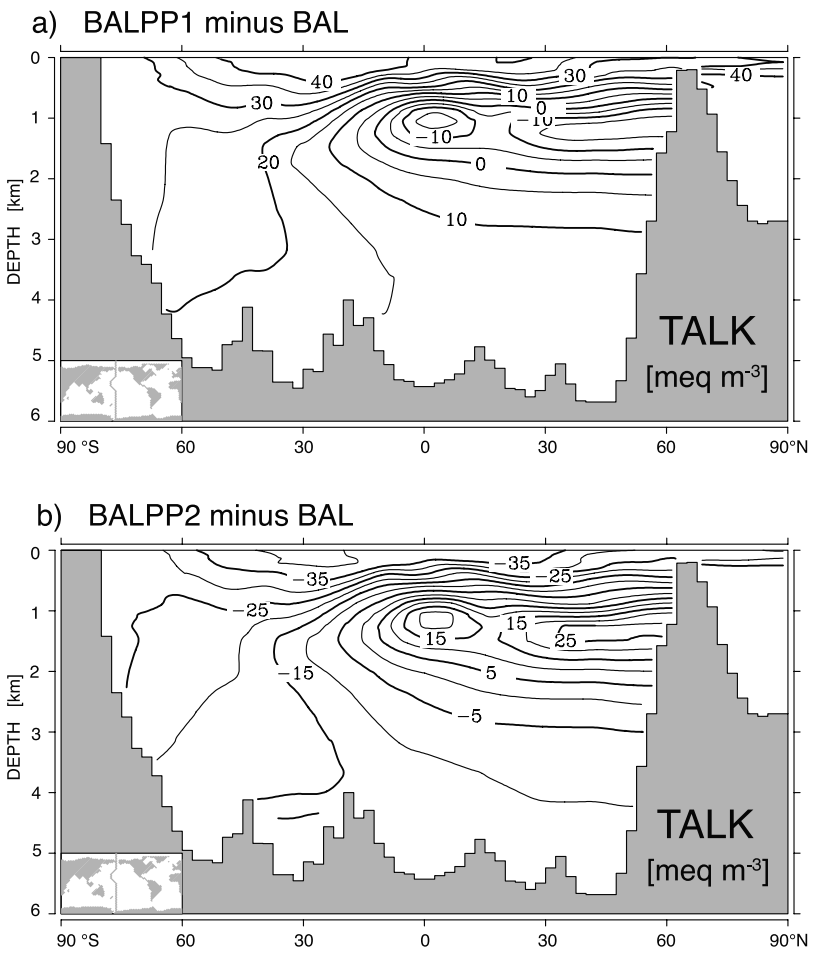

Figure 8. Alkalinity difference plots in meq m^{-3}. (a) Experiment BALPP1 minus Experiment BAL, Pacific section, 160°W. (b) Experiment BALPP2 minus Experiment BAL, Pacific section.

subtropical regions; we found that experiment BAL had lower model-data differences than the other parameterizations in the subtropical North Pacific and the subtropical North Atlantic.

[22] The differences of the various simulations from the observations as discussed in section 3 are also related to physical and biogeochemical model uncertainties as well as errors related to the data and their distribution. Physical uncertainties of the model are for example associated with the model's limitation to the resolution and eddy parameterization. In the Southern Ocean, the coarse resolution of the model can lead to an overestimate of surface nutrient supply and productivity due to too vigorous vertical mixing. Nevertheless, the general structure of the deep-sea circulation is generally reproduced well as compared with, for example, radiocarbon data [*Maier-Reimer et al.*, 1993] (see auxiliary Figure S2), CFC-11 [*Dutay et al.*, 2002], and mantle Helium-3 [*Dutay et al.*, 2004].

[23] Uncertainties related to biogeochemical parameterizations are, for example, related to the use of a singular particle size class. A refinement of the ecosystem model by a more detailed consideration of different particle size classes based on observations may improve vertical particle fluxes significantly [*Kriest*, 2002]. Particle aggregation is an important process because large aggregates have a higher sinking velocity than smaller particles. However, several parameterizations in the ecosystem model like those associated with phytoplankton growth, grazing or exudation are not well constrained by the observational evidence, which may introduce additional error in the ecosystem modeling. Our model simulations, which include ecosystem dynamics and nutrient colimitation, confirm a high sensitivity to the POC flux parameterization identified in the study of *Heinze et al.* [1999]. For example, in the POC flux parameterization of *Suess* [1980], a shallower recycling of POC is predicted by the function, leading to a strong increase in export production, which is comparable to the shallower penetration of POC and increased export production (Figure 2c) in experiment MARTIN. Overall, the consideration of a regionally varying parameterization (i.e., BAL and REFD) considerably reduces model-data differences below 2000 m (see auxiliary Table S2), but significant model-data discrepancies still exist, partially because the interannual-to-decadal variations are not considered in these simulations. In all experiments (REF, REFD, MARTIN, and BAL) the model predicts POC fluxes with the lowest model-data bias in the Atlantic ocean, subtropical North Pacific, and the Southern Ocean, but with significant differences among the different

Table 2. Modeled Export Production (g C m^{-2} yr^{-1}), Net Primary Production (NPP, g C m^{-2} yr^{-1}), and *f*-Ratio From Experiment BAL Compared With Observational Estimates Compiled by *Lutz et al.* [2002]

Region	Model Export	Obs. Export	Model NPP	Obs. NPP	Model *f*-Ratio	Obs. *f*-Ratio
Greenland and Norwegian Seas	13.20	25	80.92	86	0.16	0.29
NE Atlantic/NABE	29.66	100	248.22	252	0.12	0.40
Sargasso Sea/BATS	31.87	13	307.83	130	0.10	0.10
Subarctic Pacific/OSP	16.82	24	175.42	360	0.10	0.07
North Central Pacific gyre/HOT	12.23	25	117.86	166	0.10	0.15
South China Sea	8.17	83	66.96	151	0.12	0.55
Arabian Sea	30.87	47	199.85	460	0.15	0.10
Equatorial Pacific (±2 latitude)	51.39	32	373.31	373	0.14	0.09
Equatorial Pacific (±5 latitude)	35.75	27	257.77	281	0.14	0.10
Equatorial Pacific (±9 latitude)	21.47	15	212.72	124	0.10	0.12
Panama Basin, 82°W	40.79	36	373.57	83	0.11	0.43
Panama Basin, 86°W	4.26	36	44.72	83	0.10	0.43
Southern Ocean/Atlantic sector	28.75	22	210.99	137	0.14	0.16
NW Africa	4.00	432	39.12	720	0.10	0.60

simulations (Figures 2 and 3). Differences in POC flux estimates between the model and data have a variety of causes. One important contributor to the model-data discrepancy in POC fluxes in many areas is probably the difference between modeled export production and observational estimates (Figure 2 and Table 2). In particular, POC fluxes in BAL are predicted as a function of simulated $CaCO_3$ and opal flux and penetration depth and are therefore sensitive to production and export of POC, opal and $CaCO_3$.

[24] Observational uncertainties can be associated with significant errors in sediment trap measurement, which can result from horizontal advection of particles [*Buesseler*, 1991], "swimmers," fish or other macroscopic marine organisms that can get caught in the trap [*Hedges et al.*, 1993; *Honjo*, 1996]. Moreover, particles can degrade in traps, and differences in trapping efficiency may occur [*Yu et al.*, 2001; *Antia et al.*, 2001]. The temporal and spatial coverage of sediment trap data is still limited to a few areas, like the eastern equatorial Pacific, the North Atlantic, and the Arabian Sea, which have a significant coverage in observations (Figure 1). *Usbeck et al.* [2003] estimated particle fluxes by assimilating hydrographic data into a carbon cycle model and noted that their model tended to overestimate the observed POC fluxes by 50%, consistent with flux calibration from radionuclides, but underestimated the POC fluxes for very deep sediment traps, which is in agreement with the results of this study (see auxiliary Table S2).

5. Conclusions

[25] From the results reported in this study and from other studies it is indicated that a use of a spatially varying parameterization for particulate organic carbon fluxes yields a better representation of the observations. Overall, the geochemical distributions in the deep sea showed a high sensitivity to the selection of POC flux parameterization. Agreement between modeled POC fluxes and sediment traps below 2000 m is highest when a regionally variable POC flux parameterization is used, but significant model-data differences still exist. Regionally, the mineral ballasting parameterization for POC results in the lowest model-data differences in subtropical areas of the Atlantic and the Pacific, while the parameterization dependent on regionally variable dust input results in lowest model-data differences in the Arabian Sea. We suggest further improvement to the model by a kind of hybrid approach to POC flux modeling, using a regional and temporal variable POC flux parameterization such as mineral ballasting below 2000 m, and a different formulation for fluxes above 2000 m. This would be particularly important in areas with high dust depositions. Inverse methods with a similar approach used in the study of *Usbeck et al.* [2003], but a more detailed description of both the physical dynamics and biogeochemical cycles, would be an important future direction to provide a synthesis of the uncertainties of the models as well as the data. One example could be an improved parameterization of calcium carbonate producers. Quantifying the seasonal and spatial distribution of planktic foraminiferal fluxes reflected in sedimentary assemblages [*Zaric et al.*, 2005] may lead to a better understanding of the PIC to POC fluxes on a global scale.

[26] **Acknowledgments.** This work was supported by NASA NAG5-11245, as well as the EU JGOFS program, grant 03F0321E. In addition, thanks go to Jerry Tjiputra and Rachel Howard for reading and commenting on the manuscript.

References

Antia, A. N., et al. (2001), Basin-wide particulate carbon flux in the Atlantic Ocean: Regional export patterns and potential for atmospheric CO_2 sequestration, *Global Biogeochem. Cycles*, *15*(4), 845–862.

Archer, D., A. Winguth, D. Lea, and N. Mahowald (2000), What caused the glacial/interglacial atmospheric pCO_2 cycles?, *Rev. Geophys.*, *38*, 159–189.

Armstrong, R. A., C. Lee, J. I. Hedges, S. Honjo, and S. G. Wakeham (2002), A new, mechanistic model for organic carbon fluxes in the ocean: Based on the quantitative association of POC with ballast minerals, *Deep Sea Res., Part II*, *49*, 219–236.

Aumont, O., E. Maier-Reimer, S. Blain, and P. Monfray (2003), An ecosystem model of the global ocean including Fe, Si, P colimitations, *Global Biogeochem. Cycles*, *17*(2), 1060, doi:10.1029/2001GB001745.

Balch, W. M., H. R. Gordon, B. C. Bowler, D. T. Drapeau, and E. S. Booth (2005), Calcium carbonate measurements in the surface global ocean based on Moderate-Resolution Imaging Spectroradiometer data, *J. Geophys. Res.*, *110*, C07001, doi:10.1029/2004JC002560.

Berger, W., K. Fischer, C. Lai, and G. Wu (1987), Ocean productivity and organic carbon flux: Part I, *Tech. Rep. Ref. Ser. 87-30*, Scripps Inst. of Oceanogr., Univ. of Calif., San Diego, La Jolla.

Betzer, P. R., W. J. Showers, E. A. Laws, C. D. Winn, and G. R. DiTullio (1984), Primary productivity and particle fluxes on a transect of the equator at 153°W in the Pacific Ocean, *Deep Sea Res.*, *31*, 1–11.

Buesseler, K. O. (1991), Do upper-ocean sediment traps provide an accurate record of particle flux?, *Nature*, *353*, 420–423.

Conkright, M. E., H. E. Garcia, T. D. O'Brien, R. A. Locarnini, T. P. Boyer, C. Stephens, and J. I. Antonov (2002), *World Ocean Atlas 2001*, vol. 4, *Nutrients*, *NOAA Atlas NESDIS 52*, 392 pp., NOAA, Silver Spring, Md.

Dutay, J.-C., et al. (2002), Evaluation of ocean model ventilation with CFC-11: Comparison of 13 global ocean models, *Ocean Modell.*, *4*, 89–120.

Dutay, J.-C., et al. (2004), Evaluation of OCMIP-2 ocean models' deep circulation with mantle helium-3, *J. Mar. Syst.*, *48*, 15–36, doi:10.1016/j.jmarsys.2003.05.010.

Fischer, G., V. Ratmeyer, and G. Wefer (2000), Organic carbon fluxes in the Atlantic and the Southern Ocean: Relationship to primary production compiled from satellite radiometer data, *Deep Sea Res., Part II*, *47*, 1961–1997.

Francois, R., S. Honjo, R. Krishfield, and S. Manganini (2002), Factors controlling the flux of organic carbon to the bathypelagic zone of the ocean, *Global Biogeochem. Cycles*, *16*(4), 1087, doi:10.1029/2001GB001722.

Gardner, W., M. Richardson, and W. Smith Jr. (2000), Seasonal patterns of water column particulate organic carbon and fluxes in the Ross Sea, Antarctica, *Deep Sea Res., Part II*, *47*, 3423–3449.

Gehlen, M., C. Heinze, E. Maier-Reimer, and C. I. Measures (2003), Coupled Al-Si geochemistry in an ocean general circulation model: A tool for the validation of oceanic dust deposition fields?, *Global Biogeochem. Cycles*, *17*(1), 1028, doi:10.1029/2001GB001549.

Gieskes, J. M. (1983), The chemistry of interstitial waters of deep sea sediments: Interpretations of deep sea drilling data, in *Chemical Oceanography 8*, edited by J. P. Riley and R. Chester, pp. 221–269, Elsevier, New York.

Gruber, N., J. L. Sarmiento, and T. Stocker (1996), An improved method for detecting anthropogenic CO_2 in the oceans, *Global Biogeochem. Cycles*, *10*(4), 809–837.

Haake, B., V. Ittekkot, T. Rixen, V. Ramaswamy, R. R. Nair, and W. B. Curry (1993), Seasonality and interannual variability of particle fluxes to the deep Arabian Sea, *Deep Sea Res., Part I*, *40*, 1323–1344.

Hedges, J. I., C. Lee, S. G. Wakeham, P. J. Hernes, and M. L. Peterson (1993), Effects of poisons and preservatives on the fluxes and elemental compositions of sediment trap materials, *J. Mar. Res.*, *51*, 651–668.

Hedges, J. I., J. A. Baldock, Y. Gelinas, C. Lee, M. Peterson, and S. G. Wakeham (2001), Evidence for non-selective preservation of organic matter in sinking marine particles, *Nature*, *409*, 801–804.

Heinze, C. (2004), Simulating oceanic $CaCO_3$ export production in the greenhouse, *Geophys. Res. Lett.*, *31*, L16308, doi:10.1029/2004GL020613.

Heinze, C., E. Maier-Reimer, A. Winguth, and D. Archer (1999), A global oceanic sediment model for long-term climate studies, *Global Biogeochem. Cycles*, *13*(1), 221–250.

Heinze, C., A. Hupe, E. Maier-Reimer, N. Dittert, and O. Ragueneau (2003), Sensitivity of the marine biospheric Si cycle for biogeochemical parameter variations, *Global Biogeochem. Cycles*, *17*(3), 1086, doi:10.1029/2002GB001943.

Honjo, S. (1980), Material fluxes and modes of sedimentation in the mesopelagic and bathypelagic zones, *J. Mar. Res.*, *38*, 53–97.

Honjo, S. (1982), Seasonality and interaction of biogenic and lithogenic particulate flux at the Panama Basin, *Science*, *218*, 883–884.

Honjo, S. (1996), Fluxes of particles to the interior of the open oceans, in *Particle Flux in the Ocean*, edited by V. Ittekkot et al., pp. 91–154, John Wiley, Hoboken, N. J.

Honjo, S., and S. J. Manganini (1993), Annual biogenic particle fluxes to the interior of the North Atlantic Ocean: Studied at 34°N 21°W and 4°N 21°W, *Deep Sea Res., Part II*, *40*, 587–607.

Honjo, S., J. Dymond, R. Collier, and S. J. Manganini (1995), Export production of particles to the interior of the equatorial Pacific Ocean during the 1992 EqPac experiment, *Deep Sea Res., Part II*, *42*, 831–870.

Honjo, S., R. Francois, S. Manganini, J. Dymond, and R. Collier (2000), Particle fluxes to the interior of the Southern Ocean in the Western Pacific sector along 170°W, *Deep Sea Res., Part II*, *47*, 3521–3548.

Ittekkot, V. (1993), The abiotically driven biological pump in the ocean and short-term fluctuations in atmospheric CO_2 contents, *Global Planet. Change*, *8*, 17–25.

Kempe, S., and H. Knaack (1996), Vertical particle flux in the western Pacific below the North Equatorial Current and the Equatorial Counter Current, in *Particle Flux in the Ocean*, edited by V. Ittekkot et al., pp. 313–323, John Wiley, Hoboken, N. J.

Key, R. M., A. Kozyr, C. L. Sabine, K. Lee, R. Wanninkhof, J. L. Bullister, R. A. Feely, F. J. Millero, C. Mordy, and T. H. Peng (2004), A global ocean carbon climatology: Results from Global Data Analysis Project (GLODAP), *Global Biogeochem. Cycles*, *18*, GB4031, doi:10.1029/2004GB002247.

Klaas, C., and D. Archer (2002), Association of sinking organic matter with various types of mineral ballast in the deep sea: Implications for the rain ratio, *Global Biogeochem. Cycles*, *16*(4), 1116, doi:10.1029/2001GB001765.

Koeve, W. (2002), Upper ocean carbon fluxes in the Atlantic Ocean: The importance of the POC:PIC ratio, *Global Biogeochem. Cycles*, *16*(4), 1056, doi:10.1029/2001GB001836.

Kriest, I. (2002), Different parameterizations of marine snow in a 1D-model and their influence on representation of marine snow, nitrogen budget, and sedimentation, *Deep Sea Res., Part I*, *49*, 2133–2162.

Lutz, M., R. Dunbar, and K. Caldeira (2002), Regional variability in the vertical flux of particulate organic carbon in the ocean interior, *Global Biogeochem. Cycles*, *16*(3), 1037, doi:10.1029/2000GB001383.

Mahowald, N., K. E. Kohfeld, M. Hansson, Y. Balkanski, S. P. Harrison, I. C. Prentice, M. Schultz, and H. Rodhe (1999), Dust sources and deposition during the Last Glacial Maximum and current climate: A comparison of model results with paleodata from ice cores and marine sediments, *J. Geophys. Res.*, *104*(D13), 15,895–15,916.

Maier-Reimer, E. (1993), Geochemical cycles in an ocean general circulation model: Preindustrial tracer distributions, *Global Biogeochem. Cycles*, *7*(3), 645–677.

Maier-Reimer, E., U. Mikolajewicz, and K. Hasselmann (1993), Mean circulation of the Hamburg LSG OGCM and its sensitivity to the thermohaline surface forcing, *J. Phys. Oceanogr.*, *23*, 731–757.

Martin, J. H., G. A. Knauer, D. M. Karl, and W. W. Broenkow (1987), VERTEX: Carbon cycling in the northeast Pacific, *Deep Sea Res., Part A*, *34*, 267–285.

Mekik, F. A., P. W. Loubere, and D. E. Archer (2002), Organic carbon flux and organic carbon to calcite flux ratio recorded in deep-sea carbonates: Demonstration and a new proxy, *Global Biogeochem. Cycles*, *16*(3), 1052, doi:10.1029/2001GB001634.

Pace, M. L., G. A. Knauer, D. M. Karl, and J. H. Martin (1987), Primary production, new production and vertical flux in the eastern Pacific Ocean, *Nature*, *325*, 803–804.

Passow, U. (2004), Switching perspectives: Do mineral fluxes determine particulate organic carbon fluxes or vice versa?, *Geochem. Geophys. Geosyst.*, *5*, Q04002, doi:10.1029/2003GC000670.

Sarmiento, J. L., J. Dunne, A. Gnanadesikan, R. M. Key, K. Matsumoto, and R. Slater (2002), A new estimate of the $CaCO_3$ to organic carbon export ratio, *Global Biogeochem. Cycles*, *16*(4), 1107, doi:10.1029/2002GB001919.

Six, K. D., and E. Maier-Reimer (1996), Effects of plankton dynamics on seasonal carbon fluxes in an ocean general circulation model, *Global Biogeochem. Cycles*, *10*(4), 559–583.

Suess, E. (1980), Particulate organic carbon flux in the oceans: Surface productivity and oxygen utilization, *Nature*, *288*, 260–263.

Usbeck, R., R. Schlitzer, G. Fischer, and G. Wefer (2003), Particle fluxes in the ocean: Comparison of sediment trap data with results from inverse modeling, *J. Mar. Syst.*, *39*, 167–183.

Yu, E. F., R. Francois, M. P. Bacon, S. Honjo, A. P. Fleer, S. J. Manganini, M. M. R. VanderLoeff, and V. Ittekkot (2001), Trapping efficiency of bottom-tethered sediment estimated from intercepted fluxes of ^{230}Th and ^{231}Pa, *Deep Sea Res., Part I*, *48*, 865–889.

Zaric, S., M. Schulz, and S. Mulitza (2005), Global prediction of planktic foraminiferal fluxes from hydrographic and productivity data, *Biogeosci. Discuss.*, *2*, 849–895.

M. T. Howard and A. M. E. Winguth, Department of Atmospheric and Oceanic Sciences, University of Wisconsin-Madison, 1225 West Dayton Street, Madison, WI 53706, USA. (amwinguth@wisc.edu)

C. Klaas, Alfred-Wegener-Institut für Polar- und Meeresforschung, Postfach 12 0161, D-27515 Bremerhaven, Germany. (cklaas@awi-bremerhaven.de)

E. Maier-Reimer, Max-Planck Institut für Meteorologie, Bundesstrasse 53, D-20146 Hamburg, Germany. (maier-reimer@dkrz.de)